Neuron 51, 483–494, August 17, 2006 ©2006 Elsevier Inc. DOI 10.1016/j.neuron.2006.07.009

Neural Ensemble Coding of Satiety States

Ivan E. de Araujo,[1,4,*] Ranier Gutierrez,[1] Albino J. Oliveira-Maia,[1,5,6] Antonio Pereira, Jr.,[1] Miguel A.L. Nicolelis,[1,3,4] and Sidney A. Simon[1,2,3,4]
[1] Department of Neurobiology
[2] Department of Anesthesiology
[3] Department of Biomedical Engineering
[4] Center for Neuroengineering
Duke University Medical Center
Durham, North Carolina 27710
[5] Instituto de Histologia e Embriologia da Faculdade de Medicina
[6] Instituto de Biologia Molecular e Celular
Universidade do Porto
4200-319 Porto
Portugal

Summary

The motivation to start or terminate a meal involves the continual updating of information on current body status by central gustatory and reward systems. Previous electrophysiological and neuroimaging investigations revealed region-specific decreases in activity as the subject's state transitions from hunger to satiety. By implanting bundles of microelectrodes in the lateral hypothalamus, orbitofrontal cortex, insular cortex, and amygdala of hungry rats that voluntarily eat to satiety, we have measured the behavior of neuronal populations through the different phases of a complete feeding cycle (hunger-satiety-hunger). Our data show that while most satiety-sensitive units preferentially responded to a unique hunger phase within a cycle, neuronal populations integrated single-unit information in order to reflect the animal's motivational state across the entire cycle, with higher activity levels during the hunger phases. This distributed population code might constitute a neural mechanism underlying meal initiation under different metabolic states.

Introduction

The regulation of energy homeostasis and maintenance of stable body weight depend on the ability of the central nervous system to integrate signals reflecting the organism's current metabolic status. These signals include endocrine and peripheral cues that indicate either long-term availability of energy stores (Berthoud, 2002; Elmquist et al., 2005) or short-term, meal-related changes in metabolic state (Kissileff et al., 2003; Strader and Woods, 2005).

How does the brain integrate and process information from these multiple pathways in order to efficiently control feeding behavior? Specific patterns of change in neural activity are known to correlate robustly with fluctuations in physiological state. In particular, functional neuroimaging studies performed on humans provide clear evidence for significant decreases in brain activity in sensory and reward-related regions when initially hungry subjects reach satiety (O'Doherty et al., 2000; Small et al., 2001). Specifically, decreases in BOLD signal intensity in both human (Liu et al., 2000) and rat (Mahankali et al., 2000) hypothalamus were observed following a single administration of glucose. Consistent with these findings, electrophysiological investigations performed on alert monkeys revealed a large population of neurons in the orbitofrontal cortex (Nakano et al., 1984; Rolls et al., 1989; Yamamoto et al., 1984), amygdala (Nakano et al., 1986; Rolls, 1981), and lateral hypothalamus (Burton et al., 1976) that responded to food when the animal was hungry but not when satiated. Despite the fact that these previous studies yielded some fundamental information, they nonetheless contain at least two intrinsic limitations. First, subjects do not initiate the delivery of food, as this is controlled by the experimenter; second, these experiments are restricted to incomplete feeding cycles since they are terminated once subjects reach satiety. Thus, it is not clear whether decreased neural activity during satiety would be observed in freely feeding animals or if neural activity would return to initial levels to accompany the increases in motivation to eat that follows satiety.

Although one would expect that neuronal activity should return to its initial levels subsequent to the decreases that reflect satiation, we hypothesized that different subpopulations of neurons would account for increased activity levels during distinct hunger periods. This is because consecutive meals are not necessarily initiated under the same metabolic status (Sclafani et al., 1996; Sclafani and Springer, 1976), as given, for example, by circulating levels of insulin or glucose (Chapelot et al., 2000; Cummings et al., 2004). In order to test this hypothesis, we simultaneously recorded ensembles of single neurons in the lateral hypothalamus (LH), orbitofrontal cortex (OFC), basolateral amygdala (AM), and insular cortex (INS), while hungry rats feed themselves with sucrose to satiety (see Figure 1), across at least one complete feeding cycle (hunger-satiety-hunger). This allowed us to measure both the ability of single neurons to encode for specific phases of a feeding cycle and how neuronal populations integrate information conveyed by these phase-specific neurons in order to reflect the animal's motivational state.

Results

Feeding Behavior Consisted of One or More Feeding Cycles

Figure 2A depicts the structure of the task employed in this study. In this task, the behavioral unit of interest is defined by a set of intertrial intervals (ITIs), i.e., the set of latencies between any two consecutive episodes of licking sucrose during an experimental session. Each trial was classified as either belonging to a "hunger" or "satiety" phase, as follows: in each experimental session, start and end points for satiety phases (delimiting the hunger phases) were obtained from large impulses

*Correspondence: araujo@neuro.duke.edu

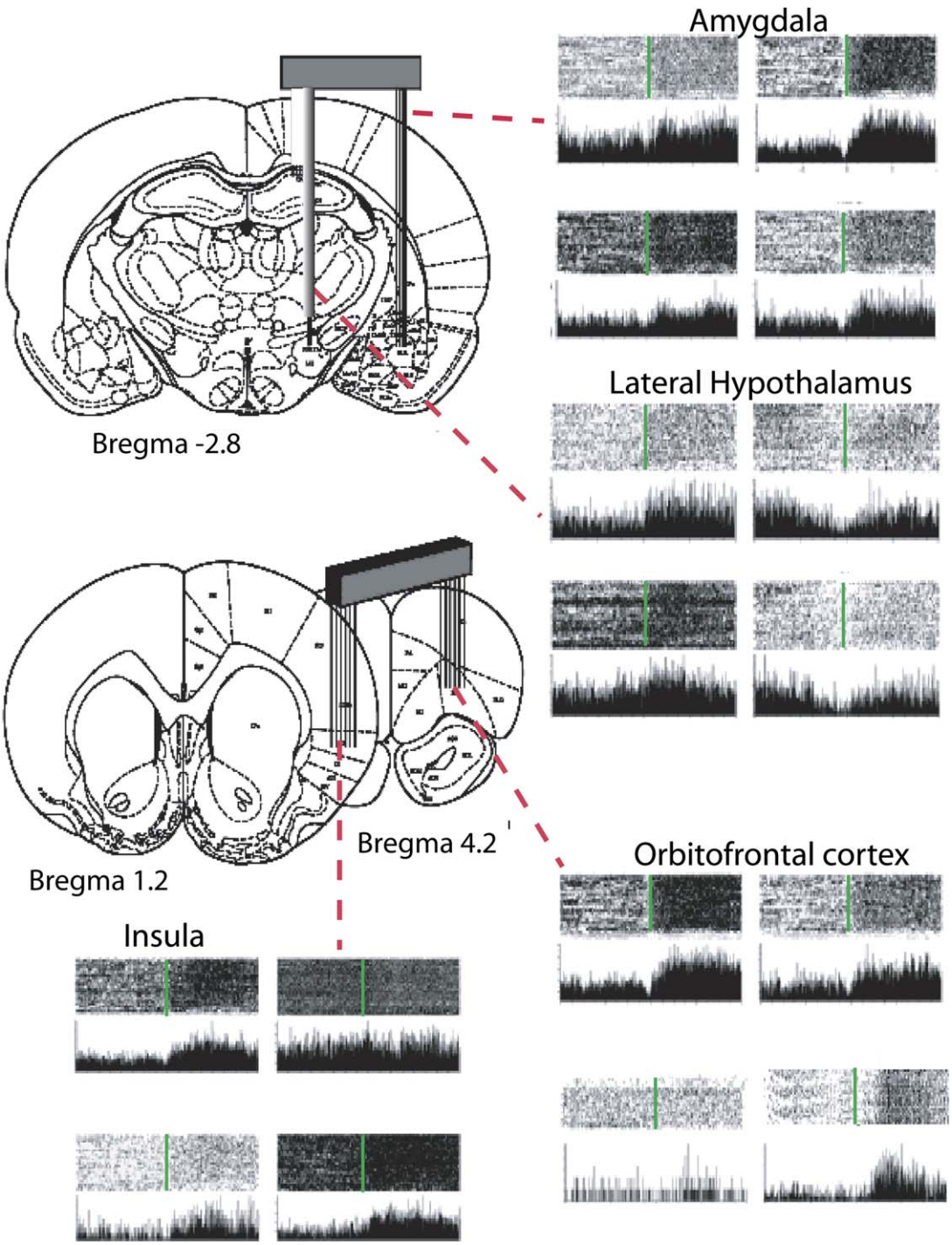

Figure 1. Multiple Simultaneous Recordings from the Gustatory-Feeding Pathways of a Behaving Rat

Schematic representation of recording sites and examples of simultaneously recorded units during sucrose intake. The upper panel shows the relative positions of microwire implants in the lateral hypothalamus and in the basolateral nucleus of the amygdala (both supported by guiding cannulae). The lower panel shows the equivalent scheme relative to the orbitofrontal cortex and insula. The dashed purple lines point to four examples in each area of perievent histograms from simultaneously recorded cells around sucrose licking (sucrose delivery indicated by vertical green line on the raster plots shown above histograms). For details on actual electrode placements, please see Figure S1.

in the derivative of the ITI function. Thus, if a specific trial is associated with a significantly large ITI derivative (see Experimental Procedures), we define this trial as the initial point of a satiety phase since even longer latencies indicate decreases in motivation to eat. Accordingly, large negative values indicate a resurge in motivation and thus denote end points for satiety phases. In a given experimental session, a set of sucrose trials consisting of two hunger phases separated by one satiety phase will be called a "feeding cycle." The relative positions

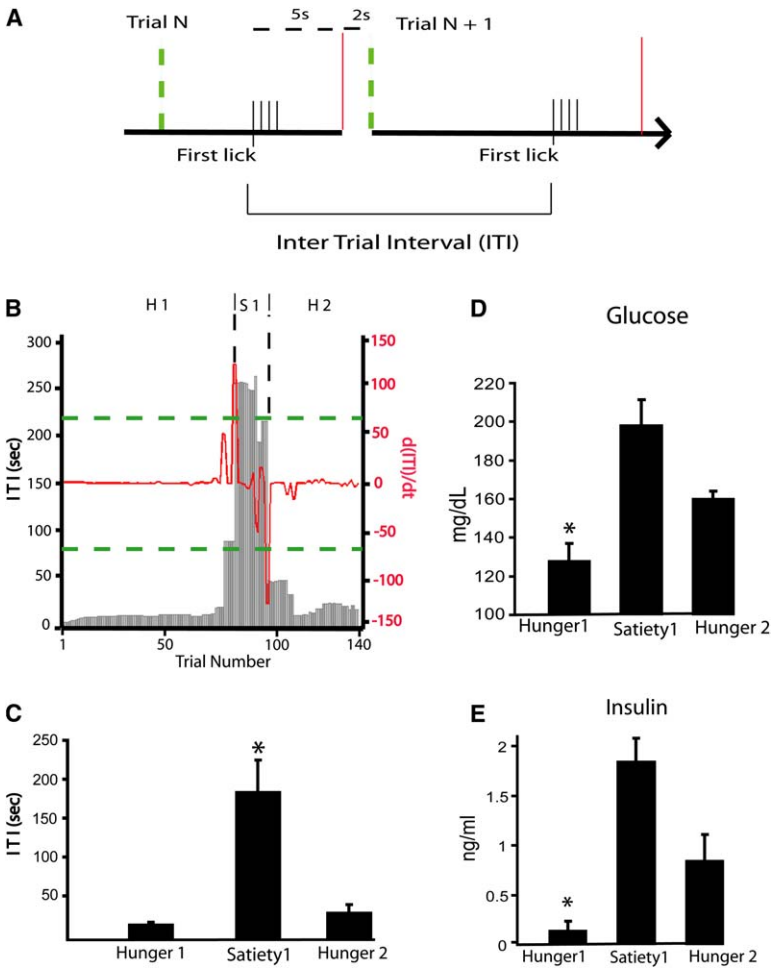

Figure 2. Behavioral Analysis and Glycemia Levels of Satiety States

(A) Scheme illustrating task structure. At a given trial n, sliding doors are open (green dashed lines), giving free access to both a sucrose solution from one of the sipping tubes and water from the second tube. Once the animal starts licking for one of the liquids, lick timestamps are recorded and doors will be closed within 5 s after the first lick in the trial (red vertical lines). Two seconds later, doors reopen and trial n + 1 starts. The animal is allowed once again access to the drinking sipping tubes. The time interval between the first lick in trial n and first lick in trial n + 1 is defined as the ITI between trials n and n + 1.

(B) Example of ITI values (gray bars) from one experimental section with two hunger phases (H1 and H2) separated by one satiety phase (S1). The red trace shows the corresponding discrete derivative of the ITIs. The positive and negative impulses in the values of the derivative crossing a prespecified threshold delimit respectively the start and end points of the satiety phase. The positive impulse indicates a rapid increase in ITI values (which we interpret as a decrease in motivation to drink sucrose) while the negative impulse implies that ITI values returned to initial (high motivation) levels. The dashed vertical lines depict satiety phase boundaries and the green dashed horizontal lines show the threshold (three standard deviations from the mean) for the derivative function.

(C) Mean ITI values during different satiety phases across experimental sessions, as obtained with the ITI derivative method. Mean ITI values are expressed in seconds, as mean ± SEM. See text for details on values.

(D) Bar graphs showing the measured glucose levels (expressed in mg/dl) across a feeding cycle. Values are expressed as mean ±SEM. See text for details on values.

(E) The same as (D) but for the case of insulin (expressed in ng/ml).

of hunger and satiety phases throughout an experiment will hereafter be indicated with numbers, such as "hunger 1," "satiety 1," "hunger 2," and so on.

Analyses of the ITIs revealed that 16/19 experimental sessions (84%) contained two distinct appetitive (hunger) phases separated by one satiety phase. The remaining three sessions (16%) contained three hunger phases (two satiety phases). An informative example of an experimental session containing two hunger phases is shown in Figure 2B, where behavior is described by ITI magnitudes. The corresponding derivative is also shown (red trace), with its significant positive and negative impulses defining the satiety phase boundaries (vertical dashed lines).

To further confirm the reliability of the method used to separate behavioral states, we measured the mean ITI value during the hunger 1 (17.8 s ± 3.0), satiety 1 (185.5 s ± 40.0), and hunger 2 (33.5 s ± 9.2) phases across experimental sessions (Figure 2C). A significant effect of feeding phase was found (Kruskal-Wallis, $p < 0.0002$), and post hoc comparisons revealed that satiety 1 values were significantly higher than both hunger 1 and hunger 2 phases (Wilcoxon signed-rank test, $p < 0.01$); however, hunger 1 and hunger 2 phases were not significantly different ($p > 0.1$). This implies that following satiety 1, animals returned to a state of high motivation to eat, a period that defined the hunger 2 state.

Microstructure of Licking Was Not Affected by Satiety States

Because the animals are moving and licking during the recording session, we were concerned that some of the recorded activity may be unassociated with motivational states. To show that this was not a critical factor in our analysis of predicting satiety, we investigated, and did not find, an effect of satiety on the *microstructure* of licking, defined here as the rhythmic licking patterns observed within 500 ms of stimulus onset. Within-session comparisons between the frequency distributions for interlick intervals (observed within 500 ms of sucrose delivery) revealed no significant differences between hunger and satiety phases ($p > 0.23$, Monte Carlo permutation tests applied to Kullback-Leibler measures, see Experimental Procedures). Peaks for the ILI distributions were 6.5 ± 0.1 Hz for hunger phases and 6.6 ± 0.08 Hz for satiety phases. We also calculated for each experimental session the mean number of licks observed within 500 ms of trial onset for both hunger and

satiety phases. Consistent with the above findings, we did not observe any difference between lick counts for hunger and satiety states (Wilcoxon signed-rank test, $p > 0.4$) within the 500 ms intervals. Mean number of licks for hunger and satiety phases were 3.27 ± 0.07 and 3.30 ± 0.06, respectively. This is consistent with previous results (Gutierrez et al., 2005) showing that the properties of licking clusters in freely licking rats are not affected by session length.

Glucose and Insulin Levels Differ between Hunger Phases

In addition to electrophysiological recordings, we also measured, in a separate group of rats implanted with jugular catheters, plasma glucose and insulin levels across the different phases of a feeding cycle. We found that levels for both factors differed across states. For glucose, measured levels were (mean ± SEM) 128.2 ± 8.8 mg/dl for hunger 1, 198.4 ± 13.1 for satiety 1, and 160.4 ± 3.8 for hunger 2 (Figure 2D). Insulin levels measured were 0.14 ± 0.08 ng/ml for hunger 1, 1.85 ± 0.22 for satiety 1, and 0.85 ± 0.25 for hunger 2 (Figure 2E). ANOVA tests revealed a significant effect of satiety phase on both glucose and insulin levels ($p < 0.004$ in both cases). In addition, direct comparisons with paired t tests between hunger phases revealed that hunger 2 yielded significantly higher glucose and insulin levels compared to hunger 1 ($p < 0.03$ in both cases). Thus, behavioral markers for the motivation to eat did not completely reflect the underlying metabolic status of the animal, and sucrose intake could be initiated under different physiological states.

Neurons in OFC, INS, AM, and Particularly in LH Are Sensitive to Changes in Satiety States

A total of 625 different single units were isolated across 19 experimental sessions. Of those, 224 (35.84%) were located in OFC, 143 (22.88%) in LH, 140 (22.40%) in INS, and 118 (18.88%) in AM. A total of 101 (16.1%) of the neurons had their firing activity significantly correlated with licking, and 152 neurons (24.32%) significantly changed their firing rate in response to the delivery of 0.7 M sucrose. Whereas the four brain areas showed similar sensitivity to oral stimulation by sucrose (Kruskal-Wallis, $p>0.3$), the majority of licking-related neurons (57 out of 101) were found in the INS.

To test for the sensitivity of single-neuron activity to changes in satiety states, for each trial the mean normalized firing rate integrated over a 1 s interval around stimulus onset (±500ms) was calculated, and then each individual trial was assigned to its corresponding satiety state (hunger 1, satiety 1, hunger 2, etc.) by using the ITI derivative criterion described above. Statistical comparisons between firing rate values (Kruskal-Wallis tests followed by Wilcoxon rank-sum tests, see Experimental Procedures for details) revealed that 179 (28.64%) neurons significantly changed their firing rates across satiety states. The majority of these units (104 out of 179 units, 58.1%) had their firing rates modulated by satiety irrespective of stimulus onset (i.e., their baseline level of activity changed across states), whereas the remaining units changed their activity across satiety states as function of stimulus onset (i.e., their baseline levels remained stable across states). No effect of brain area was found in either case (Kruskal-Wallis, $p > 0.4$). Figures 3A–3E illustrate satiety-related cells according to their responses (or absence of) to sucrose. Figure 3F shows a cell whose activity tracks the licking cycle. We have not found examples of licking-related cells that were modulated by satiety.

In what follows, the firing rate of a neuron in a given trial will be defined by its total activity around stimulus onset as above (i.e., its mean firing rate across the interval [−500 ms +500 ms] around sucrose delivery onset). In this manner, whether individual neurons produced significant responses to sucrose is not taken into account, since our effect of interest concerns changes in firing rate activity *across* trials.

We then calculated the ratio of satiety-modulated cells for each recorded brain area (number of modulated cells in area/total number of cells in area) (Figure 3G). All recorded brain structures were found to contain neurons whose firing rate was modulated by satiety. LH was found to have the highest proportion of satiety-related cells (55 neurons out of 143, 38.46% of cells modulated), followed by AM (39/118, 33.05%), INS (36/140, 25.71%), and OFC (49/224, 21.87%). There was a significant effect of brain area on the percentage of satiety modulated cells (chi-square 13.475, $df = 3$, $p < 0.004$). LH was found to be the main contributor for this association between brain region and modulation by satiety, in that the same test performed on OFC, INS, and AM resulted nonsignificant (chi-square 5.052, $df = 2$, $p > 0.08$). In addition, for each satiety-modulated cell, we determined the phase in which modulation takes effect. We found that, with respect to phase hunger 1 during satiety 1, 59 (out of 179 satiety-modulated neurons, 32.97%) decreased and 28 (15.64%) neurons increased their firing rates (type 1 and type 2 neurons, respectively). The remaining cells did not display changes during satiety 1 with respect to hunger 1; however, with respect to satiety 1, during hunger 2 a total of 21 (11.73%) cells decreased and 41 (22.90%) increased their firing rate (types 3 and 4). An additional type (type 5) will be called "bimodal," because these cells displayed a decrease in firing rate during satiety 1 and returned to their initial activity levels during hunger 2 (30 neurons, 16.76% of satiety-modulated cells). The above implies that the vast majority of satiety-modulated cells either increase or decrease monotonically their firing rates as a function of satiety states (types 1–4, 149/179 cells, 83.24%).

The ratios corresponding to each type are shown in Figure 3H and indicate that the overall neural activity remains relatively unchanged between hunger 1 and hunger 2 phases. This is supported by the results of calculating the magnitude of firing rate changes between the different phases. The mean (±SEM) firing rate change was 24.74(±3.88)% for the 117 neurons modulated between hunger 1 and satiety 1 (types 1, 2, and 5), whereas for the 92 neurons modulated between satiety 1 and hunger 2 (types 3, 4, and 5) the change was 22.99(±7.51)%, with an overall mean magnitude change of 23.86%. There was no significant difference between the magnitude of changes across the different phases ($p > 0.4$, Wilcoxon rank-sum test).

This modulation of single-cell activity by satiety was not restricted to changes in firing rate. We found that 65/625 (10.4%) of the cells displayed increases in

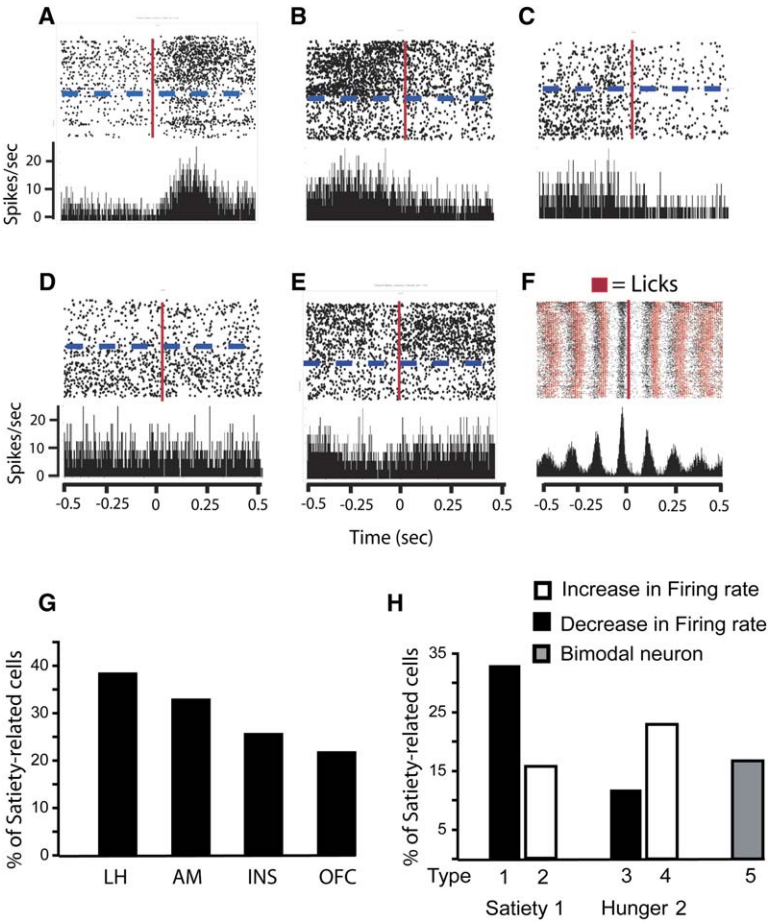

Figure 3. Examples of Single Cells Modulated by Satiety

Perievent histograms were calculated around first lick to sucrose (red vertical trace) in a trial (±500 ms). Satiety phase onsets are denoted by the horizontal dotted line in blue.

(A) Example of an LH cell whose significant response to sucrose is being reduced by satiety.

(B) Example of an AM cell in which the significant anticipatory response to sucrose decreases to baseline levels as a function of satiety phase onset.

(C) LH cell that develops a significant anticipatory response to sucrose as a function of satiety.

(D and E) Show two OFC cells that are representative of the most common type of satiety-modulated cells: increases or decreases (respectively) of basal firing rate as a function of satiety phase onset and irrespective of sucrose stimulation.

(F) Example of an INS cell in which firing rate correlates with licking activity (licks indicated by red dots).

(G) Ratio of cells modulated by satiety in each of the four recorded areas (number of cells modulated/number of cells in area).

(H) Proportion of different cell types classified according to which phase within a feeding cycle modulation by satiety occurs. Color code provides direction of change in modulation (black = increase, white = decrease, gray = bimodal), whereas the relevant satiety phase and type are shown in the x axis.

variance during satiety 1 with respect to hunger 1, while no significant changes in firing rate were detected.

Finally, we eliminated the possibility that the majority of satiety-modulated cells were contributed by a specific subgroup of animals (see Table S1 in the Supplemental Data available with this article online for number of cells recorded from each rat). We have found no significant difference, across animals, between the ratios of satiety-modulated cells (chi-square 7.109, df = 6, $p > 0.3$). Therefore, the ratio of satiety-modulated cells observed in a given experimental session is independent from which animal was being recorded.

Mean Population Firing Rates Can Represent Different Phases of a Feeding Cycle

We next investigated whether population neuronal activity could convey information on the current physiological state of the animal. For each of the 19 independent neuronal ensembles recorded during the experimental sessions, we calculated the corresponding mean population firing rates per trial. We then measured the relationship between population activity and behavioral states within a given session by calculating the correlation coefficient between the mean firing rates and the corresponding ITIs. This analysis yielded significant negative correlations in 12/19 (63%) of the sessions. Thus, in these ensembles, the mean firing rate in trial n was a good predictor of the latency magnitude to trial n + 1. These 12 ensembles were then subjected to further analyses. In what follows, we define the expression "population performance" as the absolute value of the correlation coefficient between population mean activity and the corresponding ITIs. Across the 12 relevant ensembles, the mean correlation coefficient was −0.67 (at least $p < 0.048$ in all cases with Monte Carlo permutation tests, see Experimental Procedures).

Two examples are shown in Figure 4. Figure 4A plots the mean population activity of the entire ensemble against trial numbers from its session, whereas Figure 4B shows the corresponding ITIs. (In this case, Pearson $r = -0.76$, $p < 0.002$). Figure 4C shows an example of a type 1 neuron in this ensemble; Figure 4D shows a type 4 neuron and Figure 4E depicts its only bimodal neuron (type 5) observed in this sample.

One of the sessions showing significant correlation between population activity and ITIs contained two satiety phases (and three hunger phases). The same ensemble properties seem to hold in this case, in that the satiety-modulated neurons monotonically change their firing rates according to the hunger-satiety cycle. Mean activity in population across trials is shown in Figure 4F and corresponding ITIs in Figure 4G (Pearson $r = -0.66$, $p < 0.006$). Neurons of type 1 and 2 are shown in Figures 4H and 4I.

To show that neuronal ensemble activity returned to its initial (higher) levels during hunger 2, we compared mean population firing rates between hunger 1 and hunger 2. No significant differences were found in any of the

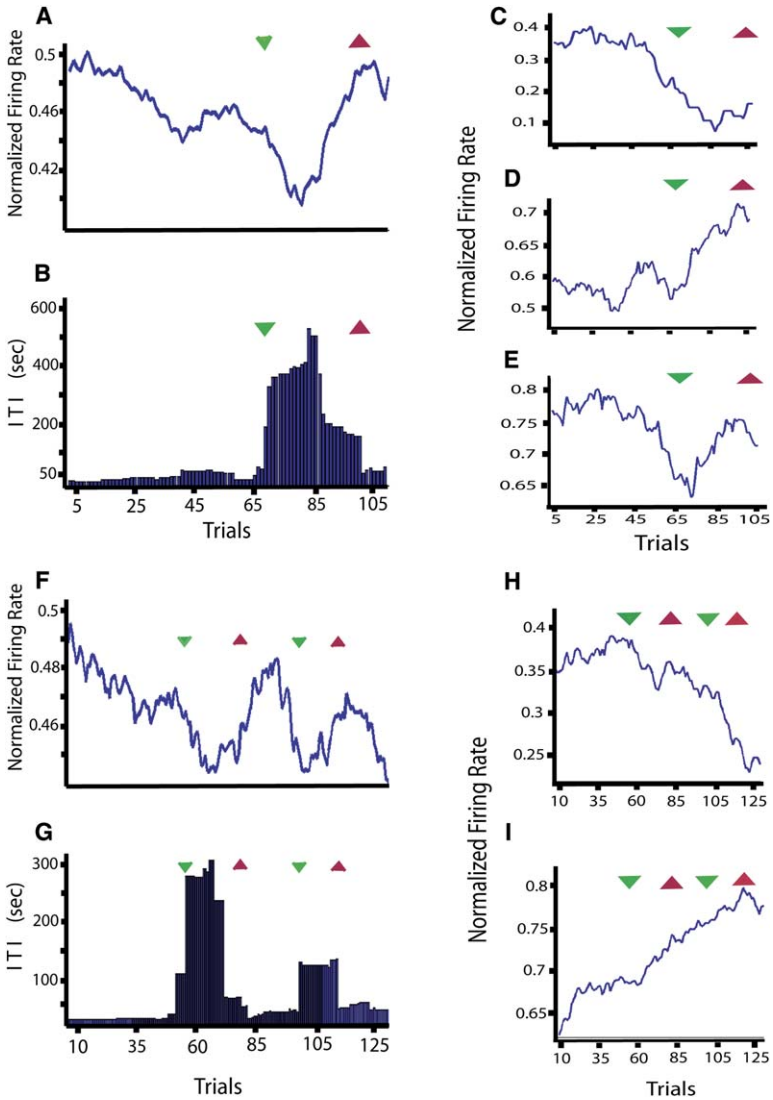

Figure 4. Examples of Experimental Sessions where the Population Mean Firing Rate Correlated Significantly with ITIs

(A) Population mean firing rate across trials throughout one experimental session. Green and red arrowheads indicate respectively start and end points for satiety phase.

(B) Corresponding ITIs for this session. Note a single significant satiety phase (large ITI values).

(C) Example of a type 1 cell from the same population.

(D) Example of a type 2 cell, again from the same population.

(E) The only bimodal neuron for this population.

(F) Population mean firing rate across trials during an experiment with two satiety phases ([G] ITIs for this session).

(H) Type 1 cell from the same population.

(I) Type 4 cell from the same population.

12 relevant sessions (Wilcoxon rank-sum test, lowest $p = 0.09$). However, higher variation of activity between trials was found during satiety 1, in that the variance-to-mean ratio is significantly higher during satiety 1 when compared to hunger 1 (Wilcoxon signed-rank test, highest $p = 0.005$). These results indicate that during satiety 1, a decrease in firing rate due to satiation was followed by a tendency of the population activity to return to its initial levels as the animal resumed feeding.

We did not find significant differences when the anticipatory (−500 ms 0 ms) and consummatory (0 ms +500 ms) periods of a trial were analyzed separately. We ascribe this result to the fact that most satiety-modulated cells (58.1%) changed their baseline levels independently of stimulus delivery.

Overall, the significant correlations reported above between population neuronal activity and ITIs imply that the boundaries, and thus duration, of satiety phases can be accurately estimated from neuronal population activity by confronting it with the discrete derivative behavioral criterion; the accuracy of this estimation is a function of the strength of the association (correlation value) between neuronal activity and ITI values.

Finally, we hypothesized that the reason for the lack of significant correlations in seven experimental sessions was the relatively low number of satiety-modulated cells in the corresponding neuronal ensembles. Indeed, out of the 434 cells recorded from the 12 ensembles showing significant correlations, 142 (32.72%) were satiety-modulated, whereas for nonsignificant ensembles only 37 out of 191 cells (19.37%) were modulated. This difference between ratios of satiety-modulated cells was found to be significant (chi-square 11.561, df = 1, $p < 0.0007$).

Mean Population Firing Rates Reflect Satiety States More Efficiently Than Individual Neurons

We next investigated whether single neurons are as efficient as neural populations (Nicolelis et al., 1998) in conveying information on satiety states. For each individual neuron belonging to an ensemble showing significant correlations, we first calculated the correlation coefficient between its activity across trials and the corresponding ITIs within a session and then computed the ratio between this coefficient and the one obtained with the original ensemble that contains this neuron. Across

the 434 neurons tested, the average ratio between individual neuron and ensemble performances was 0.24 ± 0.04. When analyses were performed as a function of brain areas, we found that LH produced on average the highest ratios (0.32 ± 0.05), followed by OFC (0.24 ± 0.03), AM (0.23 ± 0.04), and INS (0.16 ± 0.04; Figure 5A). This shows that the mean performance of individual neurons was significantly worse than the performances of the corresponding population means. Figure 5B illustrates this principle, by depicting the firing rates across trials of the satiety-modulated neurons in the ensemble shown in Figure 4A. They are ranked according to type, so that neurons 1–4 are type 1 (decrease in satiety 1), neurons 5–7 are type 4 (increase during hunger 2), and neuron 8 is type 5 (bimodal, Figure 4E). Despite the relatively low individual performances of neurons 1–7 in tracking behavioral changes (due to the monotonic properties of their modulation), when combined in a (sub-) population mean, these neurons increase their ability to reflect behavioral satiety states. Figure 5C shows the mean firing rate of monotonic neurons 1–7. This subpopulation mean closely reflects the corresponding behavioral states (Figure 4B) and greatly contributes to the significant covariation observed between the entire population mean activity (Figure 4A) and satiety. Although satiety-sensitive neurons include bimodal neurons that reflect more closely the animals' motivational state, the population's ability to reflect the animal's state does not depend on their presence (see further analyses on bimodal neurons below). In summary, the above shows that neuronal populations outperform the mean contribution to behavioral encoding of its constituent neurons, whereas single neurons seem to contain privileged information on specific phases of a feeding cycle.

Increasing Ensemble Size Improves Prediction of Satiety States

In order to assess the effect of the number of neurons in a population on performance, we randomly removed single neurons and recalculated the correlation coefficient between the resulting subpopulation and the corresponding ITIs ("Random dropping," Gutierrez et al., 2005; Narayanan et al., 2005; Wessberg et al., 2000). We found that correlation coefficient values (i.e., ensemble performance) increase with population size ($r = 0.74$; $p < 0.001$). On average, removing a single neuron from the population resulted in a decrease of 1.4% ± 0.3% in performance. This implies that even units that are not significantly modulated by satiety under our statistical criteria might contribute to population encoding of behavioral states.

Removing Neurons from LH Produces Greater Impact on Population Performance

Because performance depends on ensemble size, we calculated the ratio between the performances of region-specific ensembles and the performance of the entire original ensemble. LH produced the greatest ratios (mean ± SEM): 0.77 ± 0.06, followed by AM (0.67 ± 0.10), OFC (0.66 ± 0.16), and INS (0.35 ± 0.18; Figure 6A). Although a significant difference was found between LH and INS (Wilcoxon rank-sum, $p < 0.02$), this could simply reflect the differences between ensemble sizes. We then investigated whether there is an effect of brain area on the decrease in population performance by removing single neurons. For each of the four brain areas, we removed a single unit at a time (with substitution) and calculated the resulting correlation with the ITIs. Results are shown in Figure 6B. Removing a neuron from LH yielded an average decrease in performance of 3.8% ± 0.9%, whereas for OFC decrease was 1.1% ± 0.8%, followed by 0.4% ± 0.03% for AM and 0.1% ± 0.7% for INS. A significant effect of brain area on performance decrease was found (Kruskal-Wallis, $p < 0.03$). Post hoc comparisons (Wilcoxon rank-sum tests) revealed that LH produced a significant dropping

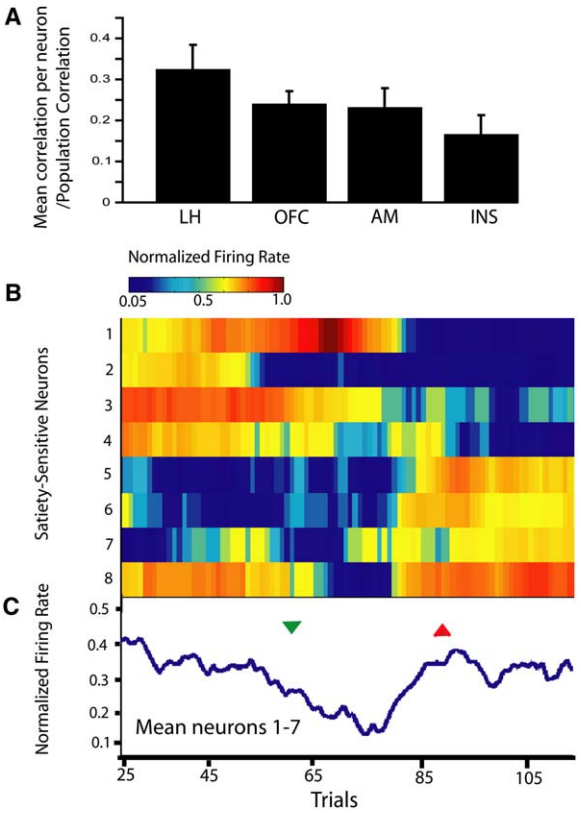

Figure 5. Performance of Individual Neurons with Respect to Neural Ensembles

(A) A plot showing the ratio between the average performance of individual neurons in a given area and the performance of the entire corresponding ensemble (performance = correlation coefficient between firing rate across trials and ITIs during the corresponding session). Analyses performed per area, showing that LH neurons carry in average more information than in other regions. However, overall performance of individual neurons is markedly inferior compared to its original population. Values are expressed as mean ± SEM.

(B) Set of satiety-modulated neurons from population shown in Figure 4A. Color code represents normalized firing rates across the session. The units were ranked according to type, so that neurons 1–4 are type 1 (decrease in satiety 1), neurons 4–7 are type 2 (increase during hunger 2), and neuron 8 is type 5 (bimodal, Figure 4E). Despite the relatively low performances of neurons 1–7 in tracking behavioral changes (due to the monotonic properties of their modulation), when combined in a (sub-) population mean, these neurons increase their ability to reflect satiety states.

(C) Mean firing rate of monotonic neurons 1–7. This subpopulation mean reflects the corresponding behavioral states (Figure 4B) and greatly contributes to the significant covariation observed between the entire population mean activity (Figure 4A) and satiety.

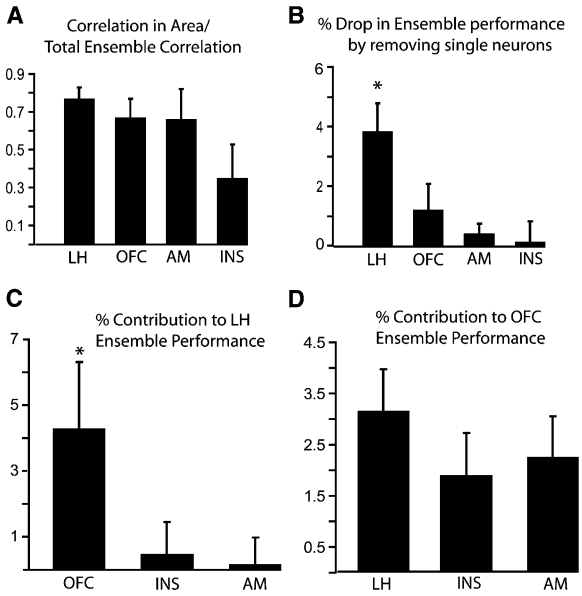

Figure 6. Relative Contributions and Interactions between the Different Recorded Brain Regions

(A) Ratio between the performances of region-specific ensembles and the performance of the entire original ensemble. The correlation coefficient obtained by restricting the analyses to each of the recorded areas was computed, and its ratio relative to the correlation coefficient obtained from the entire original ensemble is shown.

(B) To assess the contribution of each region independently of ensemble size, we measured the mean loss in performance produced by removing neurons (with substitution) from each of the recorded regions. LH is shown to be the most important contributor for ensemble performance.

(C) Mean increase in performance produced by separately adding single units from OFC, AM, and INS to LH ensembles. OFC was shown to produce the greatest increases in LH performance compared to the other three brain regions.

(D) The same analysis as in (C) but performed with respect to OFC. In this case, similar increases in OFC performance can be obtained by adding single neurons from any of the other three brain regions. Values are expressed as mean ± SEM.

in performance when compared to the other three brain areas ($p < 0.02$).

An important related issue concerns the impact on correlation values produced by removing bimodal neurons from ensembles. Across the 12 relevant sessions, we found that in average, removing a bimodal neuron results in 2.2% ± 1.8% decrease in correlation value. This value is not significantly different to the one found above to be produced by removal of LH neurons. We note that although the removal of bimodal neurons produces a greater impact on correlation values than random dropping, it did not affect the statistical significance of correlations following our significance criteria based on Monte Carlo permutation tests (see Experimental Procedures). Thus, despite the superior encoding properties of these neurons, their presence is not mandatory in populations encoding satiety states.

OFC Adds More Information to LH Ensembles Compared to the Other Brain Areas

Given the results above showing that LH neurons comparatively convey more information on satiety states, we investigated the possibility that the other brain regions might contribute differently to add information to LH ensembles. Thus, for each of the 12 significant experimental sessions, we added to the corresponding LH ensemble one single neuron from a different area at a time and computed the average increase in performance per area (Figure 6C). We found that OFC maximizes increase in LH performance (4.3% ± 2.0%), followed by INS (0.4% ± 0.9%) and AM (0.1% ± 0.8%). A significant effect of brain area on performance increase was found (Kruskal-Wallis, $p < 0.04$), with post hoc comparisons showing a greater contribution of OFC to LH performance when compared to AM and INS ($p < 0.02$). It is natural to ask whether this LH-OFC effect is reciprocal. Interestingly, although LH neurons provide nonredundant information to OFC ensembles (3.8% ± 0.8% increase in performance), the same holds for the other two brain regions (2.2% ± 0.8% for AM and 1.7% ± 0.1% for INS; Figure 6D) demonstrating that no brain area effect was significant in this case (Kruskal-Wallis, $p > 0.5$). The same result was found to hold for INS (contributions 0.06% ± 0.03%, 0.03% ± 0.01%, and 0.04% ± 0.01% from LH, OFC, and AM, respectively) and AM (0.02% ± 0.1%, 0.01% ± 0.2%, and 0.02% ± 0.1% from LH, OFC, and INS, respectively). The above implies that OFC, GC, and AM seem to form a connected circuitry sharing information on sensory and motivational aspects of feeding.

Discussion

By simultaneously recording single neurons from four different brain areas while food-deprived rats are given free access to a sucrose solution, we have shown that while neural populations reflected the overall behavioral state of the animal with decreased activity levels during satiety but not hunger phases, the large majority (83%) of satiety-modulated neurons preferentially responded to a unique phase of the feeding cycle. This specificity of single-neuron responses was likely related to changes in the internal, metabolic state of the animal across the different hunger phases (as measured by circulating glucose and insulin levels). When combined as ensembles, however, these neurons gained the ability to provide a population code that allows for predictions on the current behavioral state (hunger/satiety) of the animal by integrating information conveyed by its constituent units.

In our behavioral analyses, we used the latencies between self-initiated licking bouts ("intertrial intervals") to provide a measure for the animal's motivation to consume sucrose. These intervals directly reflect rate of consumption and therefore were used to define the boundaries between the different hunger and satiety phases. Nevertheless, the possibility remains that due to a general state of "motivational arousal" (Everitt and Robbins, 2005), additional, nonconsummatory behaviors did also display increased response rates during hunger phases. This would imply that the shorter intertrial intervals did not always reflect a state of high motivation that was specific to the ingestion of sucrose. However, the robust changes observed in glycemia levels between hunger and satiety phases (Figures 2D and 2E) strongly suggest that intertrial intervals were directly related to the homeostatic needs of the animal to consume a nutrient-rich solution.

Lower firing rate levels observed during satiety phases parallels functional neuroimaging findings of decreased activity levels in LH, OFC, AM, and INS when satiation is compared to hunger (Hinton et al., 2004; O'Doherty et al., 2000; Small et al., 2001) or thirst (de Araujo et al., 2003). In addition, studies focusing on hypothalamic responses report transient but significant decreases in activity levels following single-dose glucose administration, either orally in humans (Liu et al., 2000; Matsuda et al., 1999; Smeets et al., 2005) or systemically in rats (Mahankali et al., 2000). These changes correlated with hormonal fluctuations such as increase in insulin levels (Liu et al., 2000). Our data further extend these findings by showing an increase in neural activity toward initial levels during secondary hunger phases, likely reflecting a rise in motivation to eat that characterizes the end of a satiety phase. Thus, we provide evidence that the underlying mechanism regulating the changes in activity levels observed in functional neuroimaging studies consists of a population code distributed across different brain regions that are sensitive to changes in metabolic status.

In agreement with these functional neuroimaging studies, previous electrophysiological investigations have consistently shown that glucose-sensitive neurons in LH are generally inhibited following increases in plasma glucose levels and, reciprocally, excited by systemic doses of insulin (Bernardis and Bellinger, 1996; Oomura et al., 1974). This pattern might be functionally linked to autonomic changes accompanying hypoglycemia (Matsuda et al., 1999; Zheng et al., 2005). In addition to LH neurons that are sensitive to circulating factors, early studies in nonhuman primates have shown that a large proportion of OFC neurons change their spontaneous firing rate following eating to satiety or intravenous glucose injections (Nakano et al., 1984). Also, neurons sensitive to changes in glucose levels have been described in the monkey AM (Nakano et al., 1986). We show in the present study that populations of neurons in several brain regions involved in feeding behavior simultaneously present the same patterns of activity change across feeding cycles and thus are likely sensitive to circulating levels of metabolic factors. Specifically, we have shown that these population activity patterns result from the activity of single neurons preferentially encoding for a unique (hunger) phase of the feeding cycle.

The majority (about 58%) of satiety-modulated cells found in the present study produced changes in basal levels of activity that was dissociated from responses to sucrose, probably reflecting peripheral changes that accompany satiation. It is not clear, however, whether the remaining neurons showing modulation by satiety around sucrose delivery were also being influenced by peripheral or metabolic cues. Although we did not investigate sensory-specific satiety (O'Doherty et al., 2000; Rolls et al., 1989) as an effect in our study, it is possible that (in particular for the case of the OFC) some of the neurons showing state-dependent changes in activity were specifically modulated by the taste of sucrose. In any event, the novelty of our contribution consists in showing that satiety-modulated responses of individual neurons might differ across different feeding cycles and that only when combined as a population will single neurons gain access to neuronal processes controlling feeding behavior across several hunger-satiety phases.

We have found that when compared to the other studied brain areas, LH exhibited special sensitivity to changes in physiological state. It has been long known that lesions in LH cause drastic reductions in eating (Teitelbaum and Stellar, 1954). Besides glucose-sensitive LH neurons, it has been also shown that increases in leptin levels cause decreased activity in LH (Shiraishi et al., 1999). Increased leptin levels could thus also contribute to the decreased activations observed in the present study. We have shown in addition that neurons in OFC on average contribute most to adding information to LH subensembles. We interpret this result as meaning that neurons in OFC add little redundancy to LH ensembles (Narayanan et al., 2005) and that the OFC might be important to convey information processed in GC and AM to LH. Also, endogenous cannabinoid release is a potential mechanism signaling the current metabolic levels of the body to this LH-OFC circuit. In fact, endocannabinoid signaling has been shown to interact with circulating leptin levels (Di Marzo et al., 2001) and to modulate LH (Jo et al., 2005) and OFC (Hansson et al., 2006) processing. It is interesting to note, on the other hand, the relatively low contribution of AM to LH ensembles. As shown by the relative roles of AM and LH in conditioned potentiation of feeding (Petrovich et al., 2002), we suggest that a function of AM during eating consists in mediating the access of the hypothalamus to learned cues signaling availability of food.

Under which physiological conditions would a distributed neural coding for satiety states be the most efficient? "Hunger" and "satiety" are behavioral states prone to occur under different metabolic levels. In particular, eating can be initiated under various metabolic states (Sclafani and Berner, 1976; Sclafani and Springer, 1976), so that both energy needs and palatability are sufficient to independently elicit the same observable consummatory behaviors. This concept was corroborated by our characterization of glucose and insulin levels across feeding cycles. In particular, we found that initially hypoglycemic rats could initiate a secondary hunger phase under higher levels of circulating glucose or insulin compared to those found for the initial hunger phase (Figures 2D and 2E). Our results support the hypothesis that while single-neurons are preferentially responsive to variations in metabolic status, neural ensembles appear to integrate the information provided by these neural sensors to maintain similar levels of activity across comparable behavioral states. This distributed code acting across separate hunger phases might constitute a neural mechanism underlying meal initiation under different peripheral and metabolic environments.

Experimental Procedures

Subjects and Surgery

Seven male Long-Evans rats (Charles-Rivers) weighting 350–450 g at the time of surgery were anesthetized using 5% halothane followed by intraperitoneal injections of sodium pentobarbital (50 mg/kg) and 0.1 ml atropine sulfate. For implants in LH and AM, movable electrode bundles comprised of 16 formvar-coated tungsten wires (15 μm diameter) glued to a small microdrive and inserted into a stainless-steel guiding cannula were implanted at AP = −3.6, ML = +1.6, DV = −8.0 for LH and AP = −3.6, ML = +5.0, DV = −7.0

for AM relative to Bregma (Paxinos and Watson, 1998), and the electrodes were advanced into these areas. For OFC and gustatory cortex/INS, electrode arrays of 35 μm formvar-coated nichrome wires glued to a small microdrive were implanted at AP = +3.7, ML = +2.5, DV = −4.0 for OFC and at AP = +1.3 mm, ML = +5.2, DV = −4.5 mm relative to Bregma (Paxinos and Watson, 1998), and the electrodes were advanced into these areas. Previous to each experimental session, all arrays and bundles were advanced ~150 μm into the recorded areas by activating the microdrives, in such a way that every experimental session yielded a completely different set of units. The Duke University Institutional Animal Care and Use Committee approved all protocols.

Behavioral Task and Lick Detection

Previous to experimental sessions, animals were placed in a 22 hr water deprivation and 12 hr food deprivation schedule. All the experiments were performed in an operant box enclosed in a ventilated and sound attenuating-cubicle. Each box contained a lickometer ("V" shape, vertical slot) with a photo-beam sensor (MedAssociates) that was used to register the times when the rat's tongue contacted the drinking tubing (resolution 10 ms). Under these conditions the amount of tastant received in each lick was ~8 μl. Timestamps of licking responses and neural activity were recorded simultaneously with synchronized recordings.

Animals were allowed free access to a 0.7 M sucrose solution obtainable from one sipper tube and water from a second sipper tube. Once the animal began to lick, it was permitted access for 5 s whereupon a computer-controlled door, which blocked access to the sipper tubes, closed for 2 s and then reopened, allowing the animal to reinitiate licking. We define a "trial" as the interval between the first lick in a cluster and the closing of the doors 5 s later. The time interval between the first licks associated to two consecutive trials is called an "intertrial interval" (ITI). Experiments were allowed to run continuously for 4 hr, without external interferences on the animal's behavior. Although animals were also given free access to water during the experiments, water trials consisted of <5% of total intake and tended to concentrate within the first 3 min of each session. We did not include water trials in the analyses.

Recording Neural Activity

Simultaneous neural activity from the four brain areas was recorded from the implanted microwires and processed by using a Multineuron Acquisition Processor (Plexon Inc.) equipped with 64 channels. Only single neurons with action potentials of signal-to-noise ratios >3:1 were analyzed. The action potentials were isolated online by means of voltage-time threshold windows and a three principal components contour templates algorithm. A cluster of waveforms was assigned as a single unit only when both interspike intervals (ISI) were larger than the refractory period (set to 1.5 ms) and when the 3D projection of the first three principal components formed a visible cloud with no overlapping points with a different unit cluster. Waveforms were resorted offline and waveform alignment inspected. Only time stamps from offline-sorted waveforms were analyzed. Stability of waveform shape across a session was confirmed by using the Waveform Tracker software (Plexon Inc.).

Data Analyses

Interlick Intervals (ILIs) Distributions

Within each session, the distance between ILI distributions for hunger and satiety phases was measured with the Kullback-Leibler distance (KL distance), and significance levels were obtained by combining ILI values into a single vector that was subjected to Monte Carlo methods where positions were randomly permutated 10,000 times following an uniform distribution. Following each permutation, the resulting vector was split into two sections containing the original number of ILIs and the KL distance was recalculated. The ratio between the number of distances equal or less than the original KL distance and the total number of permutations was assigned as the p value for this comparison.

Determination of Satiety States

To determine the boundaries between satiety and hunger phases within an experimental session, the discrete derivative of the ITI series was calculated, and start points for satiety states were defined by those trials whose derivative in this point had a magnitude of three standard deviations (from the mean derivative value) units or higher (Figure 2A, dashed green line). The end point was given by the first subsequent trial whose derivative value was negative and of magnitude equal or higher than the start point magnitude (or the end of the session, whichever comes first). Hunger phases consisted of trials not falling within the satiety boundaries.

Sucrose and Licking-Related Responses

Analyses of sucrose responses in singles cells were performed on 1 s PSTHs (±500 ms) with 10 ms bins. Licking-related responses were obtained from crosscorrelograms (±500 ms) between spike and lick timestamps (10 ms bins). Confidence intervals were obtained by assuming that spike trains are Poisson trains (Abeles, 1982). Responses were considered significant whenever $p < 0.01$.

Correlation between Firing Rates and ITIs

For each single unit in a session, total spike counts in a 1 s interval around the first lick of a trial (±500 ms) was measured for each trial, and the corresponding firing-rate time series across trials was normalized to its root mean square. Mean population firing rates were obtained by averaging the normalized values across neurons with respect to each trial. Firing-rate normalization was used to assure that each neuron contributed equally to the overall population mean and that the neuron's variability across trials was being specifically measured rather than absolute values. The firing-rate series were smoothed with a causal moving-average filter of width = 5 trials. The same filter was applied to the corresponding ITI series and the Pearson correlation coefficient calculated. The first five trials (and ITIs) were not included in the computation.

Significance Tests for Correlation Coefficients

Because applying a low-pass filter to both series could itself introduce spurious correlations, we performed nonparametric significance tests to the correlation values as follows: for each firing rate series, we fixed the corresponding ITI series and applied 10,000 permutations to the raw (prefilter) firing-rate values. Following each permutation, we applied the same filter to this permutated series and calculated the corresponding Pearson correlation coefficient. The ratio between the total number of coefficients equal or less (negative correlations only) than the original Pearson coefficient and the total number of permutations was assigned as the p value for this comparison. We next repeated the same operation for the ITIs by fixing the firing-rate series. Finally, for each session we produced 10,000 series of random numbers obtained from a uniform distribution within the interval [0 1] and calculated their correlation coefficients with the ITIs, which also resulted in a p value. A correlation between population firing rates and ITIs within a session was only considered significant if the *largest* p value associated with the three permutation tests described above was *less* than 0.05.

Modulation of Single Neurons by Satiety States

Once satiety states were determined by the ITIs, modulation of single cells by states was determined by grouping trials according to their satiety phase. Then, for each neuron, comparisons between firing rates measured in each trial across satiety phases were determined with Kruskal-Wallis H tests, followed by post hoc rank-sum Wilcoxon tests. A cell was considered to be modulated by satiety whenever the post hoc rank-sum test was found to be significant at $p < 0.05$ between any two different satiety phases. To determine the direction of the significant change in these cells ("increase" versus "decrease" in firing rate), we compared the overall firing rate means values between the relevant phases.

Ensemble Analyses

By an "ensemble" we understand any subpopulation of single neurons that were recorded simultaneously. In the "random-dropping" analyses (Gutierrez et al., 2005; Narayanan et al., 2005; Wessberg et al., 2000), single neurons were removed one at a time and correlation coefficients (for correlations between populations and ITIs) were recalculated for the remaining ensemble, until its size reached one neuron. Final results for each session resulted from averages taken from 10,000 repetitions of the same random-dropping analysis. p values for positive correlations between ensemble sizes and performance were computed by transforming the correlation to create a t statistic having $n - 2$ degrees of freedom, where n is the sample size.

To calculate the contributions of different areas to LH performance, we took a single neuron from a second brain area (OFC, AM, or INS) and added this neuron to the corresponding LH ensemble

recorded during the same session. The contribution of each area was taken from the average contribution of its constituent neurons. Analogous calculations were performed for OFC, INS, and AM.

Glucose and Insulin Measurements

A separate set of five adult male (~250 g) Long-Evans rats were implanted with jugular catheters (Charles-Rivers) for blood extraction during the behavioral task. Briefly, animals are deeply anesthetized (Ketamine: Xylazine: dH_2O 2:1:10) and a small skin incision is made over the right jugular vein, with a 5 mm area of the vessel being isolated. A loose ligature is placed caudally and the cranial end of the vein is ligated. A small incision is made between the ligatures into which the catheter is inserted. A small incision is made in the scapular region to serve as exit site for the catheter, and the catheter is subcutaneously tunneled and exteriorized through the scapular incision. After 10 days recovery period, animals were placed in the same protocol as above, and blood samples were obtained through a 0.3 m polyethylene tubing connecting the catheter exit to a 1 ml syringe placed outside the behavioral box. A 500 μl blood sample was obtained for each of the behavioral phases (hunger 1, satiety 1, hunger 2) while the animal was freely behaving inside the behavioral box. Glucose measurements were performed immediately after sampling with a handheld glucometer (10 μl; Precision Xtra, Abbott Laboratories; sensitivity 20–500 mg/dl or 1.1–27.8 mmol/l). Serum was extracted from the same samples and used for insulin levels measurements with a 100%-specific rat insulin ELISA assay (100 μl, Linco Research Inc.). Data from one animal were removed from insulin analysis due to large variability between observations from the same samples, in accordance with the manufacturer's protocol. All procedures were in compliance with IACUC/Duke University regulations.

Supplemental Data

The Supplemental Data for this article can be found online at http://www.neuron.org/cgi/content/full/51/4/483/DC1/.

Acknowledgments

We thank J. Meloy for multielectrode arrays manufacturing and R. Peixoto for technical guidance on ELISA analyses. We also thank R. Costa and S. Ribeiro for valuable discussions. This work was supported by NIH DC-01065, Philip Morris USA Inc. and Philip Morris International. A.J.O.-M. is recipient of a GABBA Fellowship from FCT (Portugal).

Received: February 3, 2006
Revised: June 1, 2006
Accepted: July 10, 2006
Published: August 16, 2006

References

Abeles, M. (1982). Quantification, smoothing, and confidence limits for single-units histograms. J. Neurosci. Methods *5*, 317–325.

Bernardis, L.L., and Bellinger, L.L. (1996). The lateral hypothalamic area revisited: ingestive behavior. Neurosci. Biobehav. Rev. *20*, 189–287.

Berthoud, H.R. (2002). Multiple neural systems controlling food intake and body weight. Neurosci. Biobehav. Rev. *26*, 393–428.

Burton, M.J., Rolls, E.T., and Mora, F. (1976). Effects of hunger on the responses of neurones in the lateral hypothalamus to the sight and taste of food. Exp. Neurol. *51*, 668–677.

Chapelot, D., Aubert, R., Marmonier, C., Chabert, M., and Louis-Sylvestre, J. (2000). An endocrine and metabolic definition of the intermeal interval in humans: evidence for a role of leptin on the prandial pattern through fatty acid disposal. Am. J. Clin. Nutr. *72*, 421–431.

Cummings, D.E., Frayo, R.S., Marmonier, C., Aubert, R., and Chapelot, D. (2004). Plasma ghrelin levels and hunger scores in humans initiating meals voluntarily without time- and food-related cues. Am. J. Physiol. Endocrinol. Metab. *287*, E297–E304.

de Araujo, I.E., Kringelbach, M.L., Rolls, E.T., and McGlone, F. (2003). Human cortical responses to water in the mouth, and the effects of thirst. J. Neurophysiol. *90*, 1865–1876.

Di Marzo, V., Goparaju, S.K., Wang, L., Liu, J., Batkai, S., Jarai, Z., Fezza, F., Miura, G.I., Palmiter, R.D., Sugiura, T., and Kunos, G. (2001). Leptin-regulated endocannabinoids are involved in maintaining food intake. Nature *410*, 822–825.

Elmquist, J.K., Coppari, R., Balthasar, N., Ichinose, M., and Lowell, B.B. (2005). Identifying hypothalamic pathways controlling food intake, body weight, and glucose homeostasis. J. Comp. Neurol. *493*, 63–71.

Everitt, B.J., and Robbins, T.W. (2005). Neural systems of reinforcement for drug addiction: from actions to habits to compulsion. Nat. Neurosci. *8*, 1481–1489.

Gutierrez, R., Carmena, J.M., Nicolelis, M.A., and Simon, S.A. (2005). Orbitofrontal ensemble activity monitors licking and distinguishes among natural rewards. J. Neurophysiol. *95*, 119–133. Published online August 24, 2005. 10.1152/jn.00467.2005.

Hansson, A.C., Bermudez-Silva, F.J., Malinen, H., Hyytia, P., Sanchez-Vera, I., Rimondini, R., Rodriguez de Fonseca, F., Kunos, G., Sommer, W.H., and Heilig, M. (2006). Genetic impairment of frontocortical endocannabinoid degradation and high alcohol preference. Neuropsychopharmacology, in press. Published online February 8, 2006. 10.1038/sj.npp.1301034.

Hinton, E.C., Parkinson, J.A., Holland, A.J., Arana, F.S., Roberts, A.C., and Owen, A.M. (2004). Neural contributions to the motivational control of appetite in humans. Eur. J. Neurosci. *20*, 1411–1418.

Jo, Y.H., Chen, Y.J., Chua, S.C., Jr., Talmage, D.A., and Role, L.W. (2005). Integration of endocannabinoid and leptin signaling in an appetite-related neural circuit. Neuron *48*, 1055–1066.

Kissileff, H.R., Carretta, J.C., Geliebter, A., and Pi-Sunyer, F.X. (2003). Cholecystokinin and stomach distension combine to reduce food intake in humans. Am. J. Physiol. Regul. Integr. Comp. Physiol. *285*, R992–R998.

Liu, Y., Gao, J.H., Liu, H.L., and Fox, P.T. (2000). The temporal response of the brain after eating revealed by functional MRI. Nature *405*, 1058–1062.

Mahankali, S., Liu, Y., Pu, Y., Wang, J., Chen, C.W., Fox, P.T., and Gao, J.H. (2000). In vivo fMRI demonstration of hypothalamic function following intraperitoneal glucose administration in a rat model. Magn. Reson. Med. *43*, 155–159.

Matsuda, M., Liu, Y., Mahankali, S., Pu, Y., Mahankali, A., Wang, J., DeFronzo, R.A., Fox, P.T., and Gao, J.H. (1999). Altered hypothalamic function in response to glucose ingestion in obese humans. Diabetes *48*, 1801–1806.

Nakano, Y., Oomura, Y., Nishino, H., Aou, S., Yamamoto, T., and Nemoto, S. (1984). Neuronal activity in the medial orbitofrontal cortex of the behaving monkey: modulation by glucose and satiety. Brain Res. Bull. *12*, 381–385.

Nakano, Y., Oomura, Y., Lenard, L., Nishino, H., Aou, S., Yamamoto, T., and Aoyagi, K. (1986). Feeding-related activity of glucose- and morphine-sensitive neurons in the monkey amygdala. Brain Res. *399*, 167–172.

Narayanan, N.S., Kimchi, E.Y., and Laubach, M. (2005). Redundancy and synergy of neuronal ensembles in motor cortex. J. Neurosci. *25*, 4207–4216.

Nicolelis, M.A., Ghazanfar, A.A., Stambaugh, C.R., Oliveira, L.M., Laubach, M., Chapin, J.K., Nelson, R.J., and Kaas, J.H. (1998). Simultaneous encoding of tactile information by three primate cortical areas. Nat. Neurosci. *1*, 621–630.

O'Doherty, J., Rolls, E.T., Francis, S., Bowtell, R., McGlone, F., Kobal, G., Renner, B., and Ahne, G. (2000). Sensory-specific satiety-related olfactory activation of the human orbitofrontal cortex. Neuroreport *11*, 399–403.

Oomura, Y., Ooyama, H., Sugimori, M., Nakamura, T., and Yamada, Y. (1974). Glucose inhibition of the glucose-sensitive neurone in the rat lateral hypothalamus. Nature *247*, 284–286.

Paxinos, G., and Watson, C. (1998). The Rat Brain in Stereotaxic Coordinates (New York: Academic Press).

Petrovich, G.D., Setlow, B., Holland, P.C., and Gallagher, M. (2002). Amygdalo-hypothalamic circuit allows learned cues to override satiety and promote eating. J. Neurosci. *22*, 8748–8753.

Rolls, E.T. (1981). Responses of amygdaloid neurons in the primate. In The Amygdaloid Complex, Y. Ben-Ari, ed. (Amsterdam: Elsevier), pp. 383–393.

Rolls, E.T., Sienkiewicz, Z.J., and Yaxley, S. (1989). Hunger modulates the responses to gustatory stimuli of single neurons in the caudolateral orbitofrontal cortex of the macaque monkey. Eur. J. Neurosci. *1*, 53–60.

Sclafani, A., and Berner, C.N. (1976). Influence of diet palatability on the meal taking behavior of hypothalamic hyperphagic and normal rats. Physiol. Behav. *16*, 355–363.

Sclafani, A., and Springer, D. (1976). Dietary obesity in adult rats: similarities to hypothalamic and human obesity syndromes. Physiol. Behav. *17*, 461–471.

Sclafani, A., Lucas, F., and Ackroff, K. (1996). The importance of taste and palatability in carbohydrate-induced overeating in rats. Am. J. Physiol. *270*, R1197–R1202.

Shiraishi, T., Sasaki, K., Niijima, A., and Oomura, Y. (1999). Leptin effects on feeding-related hypothalamic and peripheral neuronal activities in normal and obese rats. Nutrition *15*, 576–579.

Small, D.M., Zatorre, R.J., Dagher, A., Evans, A.C., and Jones-Gotman, M. (2001). Changes in brain activity related to eating chocolate: from pleasure to aversion. Brain *124*, 1720–1733.

Smeets, P.A., de Graaf, C., Stafleu, A., van Osch, M.J., and van der Grond, J. (2005). Functional MRI of human hypothalamic responses following glucose ingestion. Neuroimage *24*, 363–368.

Strader, A.D., and Woods, S.C. (2005). Gastrointestinal hormones and food intake. Gastroenterology *128*, 175–191.

Teitelbaum, P., and Stellar, E. (1954). Recovery from the failure to eat produced by hypothalamic lesions. Science *120*, 894–895.

Wessberg, J., Stambaugh, C.R., Kralik, J.D., Beck, P.D., Laubach, M., Chapin, J.K., Kim, J., Biggs, S.J., Srinivasan, M.A., and Nicolelis, M.A. (2000). Real-time prediction of hand trajectory by ensembles of cortical neurons in primates. Nature *408*, 361–365.

Yamamoto, T., Oomura, Y., Nishino, H., Aou, S., Nakano, Y., and Nemoto, S. (1984). Monkey orbitofrontal neuron activity during emotional and feeding behaviors. Brain Res. Bull. *12*, 441–443.

Zheng, H., Patterson, L.M., and Berthoud, H.R. (2005). Orexin-A projections to the caudal medulla and orexin-induced c-Fos expression, food intake, and autonomic function. J. Comp. Neurol. *485*, 127–142.